Available online at www.sciencedirect.com

SCIENCE DIRECT®

International Journal of Thermal Sciences 45 (2006) 180–189

International Journal of Thermal Sciences

www.elsevier.com/locate/ijts

Modeling convective drying of ventilated wall chambers in building enclosures

Danko Davidovic [a], Jelena Srebric [a,*], Eric F.P. Burnett [b]

[a] *Department of Architectural Engineering, Pennsylvania State University, University Park, PA 16802, USA*
[b] *Departments of Civil and Environmental Engineering and Architectural Engineering, Pennsylvania State University, University Park, PA 16802, USA*

Received 21 October 2004; accepted 10 June 2005

Available online 14 July 2005

Abstract

In North America, residential enclosure walls are often built with provision for natural convection and, therefore, provide potential for ventilation drying within the wall. At present, our knowledge of the drying process in the wall systems is limited. The drying process is driven by very low airflow rates with complex flow patterns through the narrow and irregular wall cavities, resulting mostly in unstable ventilation driven by natural convection. Different venting strategies coupled with the stochastic nature of driving forces for ventilation contribute to the complexity of the drying process. Both the physical and the mathematical modeling of wall cavity convective drying are challenging. However, it is difficult to accurately predict the convective drying rates in wall cavities at any time during the year. Nevertheless, the convective drying process is probably one of the key mechanisms for mold suppression in residential walls in the US, and therefore, needs to be fully understood and quantified.

An equation is developed to estimate the convective moisture transport in screened and ventilated wall systems. The intent was to develop a simple equation for practical design applications. The equation represents a solution of the two-dimensional moisture transport equation, solved for steady state conditions assuming laminar flow with a uniform velocity field in the wall cavity.

The results derived from the simple equation were compared to measured data obtained in the Building Enclosure Test Laboratory (BeTL) at the Pennsylvania State University (PSU). The comparison showed that the simple equation can accurately predict the convective drying rates. The results are highly sensitive to the environmental conditions in the immediate vicinity of the wet wall surfaces. This equation could be used in engineering practice to provide an estimate of convective drying rates in the ventilated chamber of rain-screened and ventilated wall systems. Future validation with on-site experiments is necessary.

Keywords: Ventilated chamber; Enclosure wall; Natural convection; Ventilation; Convective drying rate; Parametric correction function; Effective wetting surface area coefficient

1. Introduction

The deterioration of materials and human health in buildings due to the presence of moisture in building walls has been the focus of many studies. Although many characteristics of moisture transport have already been defined, there is still a need to understand the nature of convective transport and the control of moisture within and across building enclosures. Therefore, a study of the potential for convective moisture removal from building enclosures is of great importance for many engineers, architects, building owners and manufacturers involved in the design, construction and operation of buildings, particularly low-rise residential buildings. A screened and ventilated wall system, commonly used in North America, is presented in Fig. 1.

Ventilated enclosure wall systems have three basic components:

(1) a screen (brick, masonry or vinyl siding);

* Corresponding author.
E-mail address: jsrebric@psu.edu (J. Srebric).

1290-0729/$ – see front matter
doi:10.1016/j.ijthermalsci.2005.06.002

Nomenclature

A	$= W\delta$ ventilated chamber cross sectional area	m^2
C	$\approx \frac{0.622}{p_{atm}}$ constant	Pa^{-1}
D	diffusion coefficient	$m^2 \cdot s^{-1}$
H	height of the ventilated chamber	m
$\dot{m}_{AIR}$	mass flow rate of the air	$kg \cdot s^{-1}$
p	air pressure	Pa
p_{atm}	atmospheric pressure	Pa
p_v	partial water vapor pressure in the air	Pa
$p_{v,s}$	partial water vapor pressure of saturation	Pa
$\dot{Q}$	volumetric flow rate of air	$l \cdot s^{-1}$
$\dot{S}_M$	bulk mass source	$kg \cdot s^{-1}$
T	air temperature	K
u	horizontal velocity component	$m \cdot s^{-1}$
V	$= \frac{\dot{m}_{AIR}}{\rho A}$ uniform inlet velocity ($V = \text{const}$)	$m \cdot s^{-1}$
v	vertical velocity component	$m \cdot s^{-1}$
W	width of the ventilated chamber	m
w	humidity ratio	$kg \cdot kg_{dry,air}^{-1}$

Greek symbols

δ	wall cavity depth	m
μ	water vapor permeability in the air ($\mu = 1.7 \times 10^{-10}$ s)	s
ρ	moist air (bulk) density	$kg \cdot m^{-3}$
ρ_k	density of kth component	$kg \cdot m^{-3}$
λ_n	$= \frac{(2n+1)}{2\delta} \cdot \pi$ characteristic value, $n = 0, 1, 2, \ldots$	

Superscripts and subscripts

AIR	air
atm	atmospheric
k	kth component
M	mass
n	index
v	vapor
s	saturation
wall	wall surface

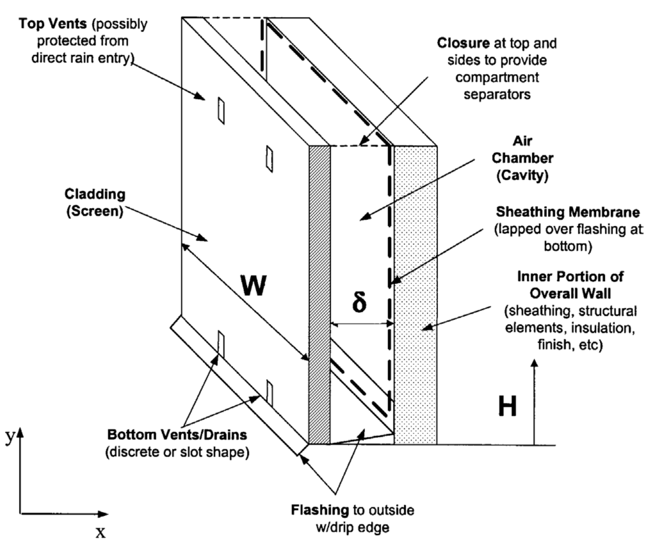

Fig. 1. Representative rain-screened and ventilated wall system.

(2) an air chamber sealed from the building interior;
(3) vent openings, connecting the ventilated wall chamber with the exterior environment (through the screen).

Among the various processes of moisture transfer and moisture storage within and across the building enclosure, convective water vapor transfer, i.e., moisture removal by airflow through the ventilated wall system, is of particular interest. This mechanism is one of the least studied, but its contribution to the overall wall-drying process is significant [1]. An accurate estimate of the convective drying rate is needed to avoid moisture-related problems such as mold growth or corrosion. Moisture within the building enclosure can also cause structural problems, and moreover, it may have serious effects on the health of occupants. Therefore, an estimate of the potential for convective drying in ventilated wall systems is important.

A comprehensive study of moisture transport within a building enclosure should consider the following [1]:

- the nature and availability of moisture sources,
- the mechanisms of moisture storage,
- the transport processes for moisture removal, and
- the materials used in multi-layer wall assembly and their hydrothermal properties.

The focus of this study is the convective transport process for moisture removal assuming the other factors to be known. The basic equations for the moisture-transport mechanisms in liquid and vapor phases through porous media, for the sorption processes with phase changes at the surface layers, and for convective transport at the surface are available in Refs. [2–4]. However, the complexity of the governing equations that describe these processes requires the use of numerical methods to solve the mathematical model [5]. Thus, an accurate prediction of convective moisture removal from a ventilated wall system requires knowledge of the hydrothermal properties of building materials, an adequate model of the transport processes, and efficient numerical solution techniques. One objective in this study is to establish a simpler approach for the prediction of ventilation drying.

2. Theoretical derivation of the model equation

The main objective of this study is to develop a single expression to model the convective drying in screened and ventilated building enclosure systems. The equation should have a relatively simple form, in order to be widely accepted.

The drying process in the ventilated chamber, shown in Fig. 1, is approximated as two-dimensional. This assumption is based on the experimental smoke visualization and numerical computational fluid dynamic calculations available in Ref. [6]. In addition, changes in the convective drying rate along the width of the chamber W may be considered negligible [1]. The general transport equation for convective mass transfer in Cartesian coordinates for a kth "species" in two dimensions for steady-state flow in a multiphase system ($\partial/\partial t = 0$, $\partial/\partial z = 0$, $w = 0$) has the following form [7]:

$$\rho u \frac{\partial \rho_k}{\partial x} + \rho v \frac{\partial \rho_k}{\partial y} = \rho D \frac{\partial^2 \rho_k}{\partial x^2} + \rho D \frac{\partial^2 \rho_k}{\partial y^2} + \dot{S}_M \tag{1}$$

where the kth component represents the water vapor in this case. Diffusion along the height ($\frac{\partial^2 \rho_k}{\partial y^2} \ll \frac{\partial^2 \rho_k}{\partial x^2}$) and driving forces due to thermo-diffusion and pressure-diffusion effects may be neglected because of the dominance of mass transport due to convection in the vertical direction. Velocities in the horizontal direction are assumed to be negligible compared to velocity in the vertical direction ($u \ll v$). Consequently, the convective term denoting mass transport in the horizontal direction may be omitted from the analysis ($\rho u \frac{\partial \rho_k}{\partial x} \ll \rho v \frac{\partial \rho_k}{\partial y}$). If it is assumed that there is initially no mass source of water vapor in the air within the chamber, then $\dot{S}_M = 0$. In other words, the moisture phase changes, e.g., evaporation and condensation, are not likely to occur within the bulk volume of the chamber except on the wall surface. Finally, Eq. (1) reduces to:

$$\rho v \frac{\partial \rho_k}{\partial y} = \rho D \frac{\partial^2 \rho_k}{\partial x^2} \tag{2}$$

In order to solve Eq. (2), it is necessary to define the velocity profile across the wall chamber. The airflow through the entire ventilated chamber is assumed to be laminar. Experiments on real wall systems performed by Saelens and Hens [8] showed that velocities in the wall chamber caused by natural ventilation driving forces are so small that a laminar flow regime is a correct assumption for most of the time during a year. The velocity profile in the wall chamber may be considered the same as for the flow between two infinite parallel plates because of the large aspect ratio of the chamber. Therefore, the flow in the ventilated chamber can be approximated with flow between two infinite parallel plates. In fluid-mechanics theory, this type of flow develops from a uniform to a fully developed parabolic laminar profile due to the action of viscous forces. The development of the flow between infinite parallel plates is presented in Fig. 2.

The length of the hydrodynamic entry region depends on the Reynolds number and the hydraulic diameter. However, the same approach may not produce accurate results for the entry length in a ventilated chamber due to the complex inlet velocity conditions in and the specific chamber geometry. To avoid difficulties in accurately predicting particular regions, it is recommended that the average velocity across the cavity v_{ave} be used. This value is equal to two-thirds of the maximum velocity at the center of the cavity for fully developed laminar flow between two infinite parallel plates ($v_{\text{ave}} = \frac{2}{3} v_{\max}$ for $x = \delta/2$). Therefore, a uniform and unidirectional velocity profile may be assumed ($u = 0$, $v = v_{\text{ave}} = V = \text{const}$). In other words, the velocity is perpendicular to the wall cavity cross-section. Strictly speaking, this assumption is valid only at the entrance region. Moreover, the parabolic velocity profile in fully developed laminar flow would introduce more complexity to the solution procedure. Even with the simple, uniform-velocity profile, the analytical solution has a relatively complex form (shown later). It is still possible to obtain the solution for the parabolic velocity profile in closed form, but it is usually expressed in terms of the Graetz function. The final expression of the solution may be found in [5]. However, this literature source does not provide any information about evaluating the Graetz function. Moreover, the standard computer tools available do not include this function by default.

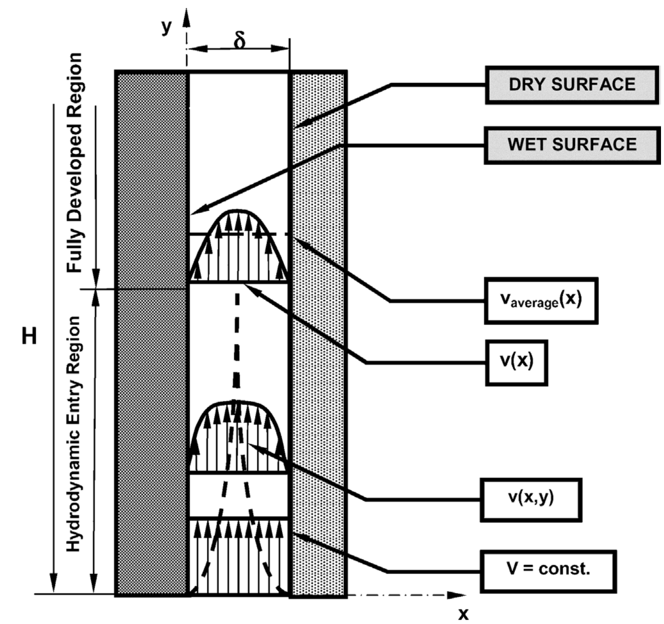

Fig. 2. Development of the velocity profile for laminar flow inside a wall chamber.

In light of all these considerations, a simple uniform velocity field will be considered in our model. The velocity defined in this way represents the averaged value of velocity, and it is equal to two-thirds of maximum velocity at the center of the cavity for the fully developed laminar velocity profile as denoted in Fig. 2.

Besides the velocity field assumption, Eq. (2) also needs an assumption for the density of the water vapor (ρ_k). In moisture transport studies, it is common to express the density of water vapor in terms of humidity ratios or partial water vapor pressures in the air. The relation that connects these two variables is:

$$w = 0.622\frac{p_v}{p_{\text{atm}} - p_v} \tag{3}$$

The partial pressure of the water vapor p_v strongly depends on the local temperature. Although the wall temperature may significantly vary over the wall surface, this variation is ignored in the steady-state model, and the surface temperature of the wall cavity in the flow direction is assumed to be uniform ($T_{\text{wall}} = \text{const}$). Another crucial assumption in the model is that the wall surface is fully wetted. In other words, the partial pressure of water vapor at the wall surface is equal to the saturation pressure of water vapor for the moist air:

$$p_v(x = \delta) = p_{v,\text{sat}}(T_{\text{wall}}) \tag{4}$$

Then, the humidity ratio of the air at the wall cavity surface can be expressed as:

$$w_{\text{sat}}(T_{\text{wall}}) = 0.622\frac{p_{v,\text{sat}}(T_{\text{wall}})}{p_{\text{atm}} - p_{v,\text{sat}}(T_{\text{wall}})} \tag{5}$$

The values of partial water–vapor pressures in the moist air and at the wall surfaces (p_v, $p_{v,\text{sat}}$) are relatively small compared to the atmospheric pressure ($p_v, p_{v,\text{sat}} \ll p_{\text{atm}}$). Accordingly, the following expression may be adopted:

$$\frac{w}{w_{\text{sat}}(T_{\text{wall}})} \approx \frac{p_v}{p_{v,\text{sat}}(T_{\text{wall}})} \tag{6}$$

The partial water–vapor-pressure ratios in the air and at the wall cavity surfaces are proportional to the humidity ratios. Therefore, according to Eq. (3), the following relation can be derived:

$$w = Cp_v \tag{7}$$

where

$$C \approx \frac{0.622}{p_{\text{atm}}} = \text{constant} \tag{8}$$

A similar approximation was developed by TenWolde [10]. For a fully developed laminar flow regime through the wall chamber, the total air pressure drop (an order of magnitude of several Pascals) is negligible compared to the static pressure of the airflow. Therefore, the assumption expressed by Eqs. (7) and (8) is valid for most engineering calculations. Consequently, the density of the water vapor (ρ_{k}) is directly proportional to the partial pressure of water vapor, and Eq. (2) may be transformed in the following way:

$$\rho CV\frac{\partial p_v}{\partial y} = \mu\frac{\partial^2 p_v}{\partial x^2} \tag{9}$$

The thermo-physical properties of the air, bulk density, and water vapor permeability are assumed to be independent of temperature and pressure. The atmospheric pressure is assumed to be the same as the barometric pressure at sea level. All of the necessary assumptions are introduced, and Eq. (9) represents the moisture transport equation that needs to be solved analytically. The boundary conditions associated with the model presented, Eq. (9), are:

(1) $p_v(x, y = 0) = p_{v,\text{IN}}$ (10)

(2) $p_v(x = 0, y) = p_{v,S}(T_{\text{wall}})$ (11)

(3) $\dfrac{\partial p_v(x = \delta, y)}{\partial x} = 0$ (12)

The first two boundary conditions define the water–vapor pressure at the inlet and in the air layer adjacent to the wet wall surface. In other words, the wet wall surface is considered to be fully wetted, and the air in contact with the surface is saturated. The third boundary condition states that no water vapor transport occurs through the dry wall face of the wall system. This surface is considered to be impermeable to moisture transport. This assumption may be valid for the cases where a water vapor retarder is attached to one of the ventilated chamber walls. It may also be valid for vinyl siding cladding walls, if no air infiltration is assumed to take place through the cladding wall. The profile of the water–vapor pressure across the cavity and the corresponding boundary conditions for the model described above are presented in Fig. 3.

The model presented above is also applicable to a case where the wet face wall surface and moisture source are on the right-hand side while the dry wall surface is on the left side. This scenario may occur for the rain penetrated moisture through the brick veneer or vinyl siding cladding wall systems. In that case, the inner portion of the wall system is covered with water–vapor retarder, preventing the moisture transport towards the building interior space.

The saturation water vapor pressure in the air $p_{v,S}$ can be approximated as a function of wall cavity surface temperature T_{wall}. Many correlations are available to describe this relationship. For example, relatively simple equations are found in Refs. [4,11]. In our model, the simpler expression is adopted [4]:

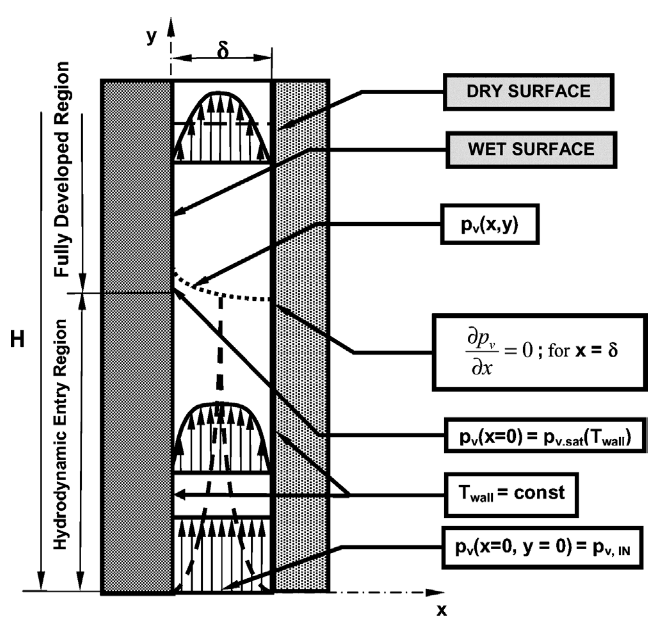

Fig. 3. Boundary conditions for the moisture transport model in ventilated chamber.

$$p_{v,\mathrm{sat}}(T_{\mathrm{wall}}) = \exp\left(A + \frac{B}{T_{\mathrm{wall}}} + \frac{C}{T_{\mathrm{wall}}^{3/2}}\right) \tag{13}$$

where the constants are: $A = 22.565$; $B = -2377.1$ [K]; $C = -33623$ [$\mathrm{K}^{1.5}$].

In order to make the boundary conditions homogeneous, the following pressure variables are defined as:

$$\tilde{p} = p_v - p_{v,S}(T_{\mathrm{wall}})$$

$$\tilde{p}_{\mathrm{IN}} = p_{v,\mathrm{IN}} - p_{v,S}(T_{\mathrm{wall}})$$

The transformed form of the model Eq. (9) and accompanying boundary conditions Eqs. (10)–(12) are:

$$\rho C V \frac{\partial \tilde{p}}{\partial y} = \mu \frac{\partial^2 \tilde{p}}{\partial x^2} \tag{14}$$

$$\tilde{p}(x, y = 0) = \tilde{p}_{v,\mathrm{IN}} \tag{15}$$

$$\tilde{p}(x = 0, y) = 0 \tag{16}$$

$$\frac{\partial \tilde{p}(x = \delta, y)}{\partial x} = 0 \tag{17}$$

Eqs. (14)–(17) describe the physical model for the moisture transport in the wall chamber. Eq. (14) is classified as a steady-state, parabolic, linear, second-order, partial differential equation with homogeneous boundary conditions and constant coefficients.

Various solution techniques are available to solve these types of equations, such as separation of variables, integral transforms, transformations of dependent variables, and similarity transformations [12]. The similarity transformations and separation of variables are the two most widely used methods to solve the problems of heat conduction [13,14]. The similarity transformations have several characteristics that may create difficulties in solution procedures. Most importantly, the process of variable transformation strongly depends on the selected similarity variables. Moreover, the proper choice of similarity variable requires extensive scientific experience and knowledge. Therefore, the method of variable separation has been chosen to solve Eqs. (14)–(17). The methodology for solving partial differential equations using separation of variables is available in the literature [9,15,16]. The step-by-step solution procedure, extracted from the literature and slightly modified for this particular model, is also available in a published thesis [6]. The final solution is the following expression for the dimensionless ratio of partial water–vapor pressures for the air in the wall cavity and inlet opening:

$$\frac{\tilde{p}(x, y)}{\tilde{p}_{\mathrm{IN}}} = \frac{2}{\delta} \sum_{n=0}^{\infty} e^{-\frac{\lambda_n^2 \cdot \mu}{\rho \cdot C \cdot V} \cdot y} \frac{\sin(\lambda_n x)}{\lambda_n} \tag{18}$$

where: $\tilde{p}(x, y) = p_v(x, y) - p_{v,S}(T_{\mathrm{wall}})$ and $\tilde{p}_{\mathrm{IN}} = p_{v,\mathrm{IN}} - p_{v,S}(T_{\mathrm{wall}})$.

However, this expression (Eq. (18)) is still inconvenient for practical use. Therefore, it is assumed that a representative value for partial water–vapor pressure at the outlet opening may be obtained by averaging the integral across the wall cavity and dividing by the wall cavity depth, δ, i.e.:

$$\frac{\tilde{p}(y)}{\tilde{p}_{v,\mathrm{IN}}} = \frac{1}{\delta} \int_0^{\delta} \frac{2}{\delta} \sum_{n=0}^{\infty} e^{-\frac{\lambda_n^2 \cdot \mu}{\rho \cdot C \cdot V} \cdot y} \frac{\sin(\lambda_n x)}{\lambda_n} \, \mathrm{d}x \tag{19}$$

Then, Eq. (18) becomes:

$$\frac{\tilde{p}(y)}{\tilde{p}_{v,\mathrm{IN}}} = \frac{2}{\delta^2} \sum_{n=0}^{\infty} \frac{e^{-\frac{\lambda_n^2 \mu p_{\mathrm{atm}} A}{0.622 \dot{m}_{\mathrm{AIR}}} \cdot y}}{\lambda_n^2} \tag{20}$$

or

$$\frac{p_v(y) - p_{v,S}(T_{\mathrm{wall}})}{p_{v,\mathrm{IN}} - p_{v,S}(T_{\mathrm{wall}})} = \frac{2}{\delta^2} \sum_{n=0}^{\infty} \frac{e^{-\frac{\lambda_n^2 \mu p_{\mathrm{atm}} A}{0.622 \dot{m}_{\mathrm{AIR}}} \cdot y}}{\lambda_n^2} \tag{21}$$

Eq. (21) permits evaluation of the water–vapor partial pressure distribution, but it does not predict the drying rates. The convective drying rate or the water vapor mass flux through the wall chamber can be calculated using the following formula:

$$\Delta \dot{m}_{\mathrm{DRY}} = \dot{m}_{\mathrm{AIR}} \big[w(y = H) - w_{\mathrm{IN}} \big] \tag{22}$$

or, in terms of the partial water–vapor pressures in the air:

$$\Delta \dot{m}_{\mathrm{DRY}} = 0.622 \dot{m}_{\mathrm{AIR}} \left[\frac{p_v(y = H)}{p_{\mathrm{atm}} - p_v(y = H)} - \frac{p_{v,\mathrm{IN}}}{p_{\mathrm{atm}} - p_{v,\mathrm{IN}}} \right] \tag{23}$$

By the substitution of Eq. (21) in Eq. (23), and introduction of an additional parametric function Φ (to be later defined in more details):

$$\Phi = f(\textit{geometry of the chamber}, \dot{m}_{\mathrm{AIR}}, \text{air } \textit{thermophysical properties}) \tag{24}$$

Eq. (23) takes a relatively simple form for estimating the convective drying rate:

$$\Delta \dot{m}_{\mathrm{DRY}} = \dot{m}_{\mathrm{AIR}} \left[0.622 \frac{p_{v,S}(T_{\mathrm{wall}}) + \Phi \Delta p}{p_{\mathrm{atm}} - p_{v,S}(T_{\mathrm{wall}}) - \Phi \Delta p} - W_{\mathrm{IN}} \right] \tag{25}$$

where Φ is the parametric correction function and $\Delta p = p_{v,\mathrm{IN}} - p_{v,S}(T_{\mathrm{wall}})$ is the difference between the partial water vapor at the air inlet and saturated wall surface. This pressure differential is the driving force for convective moisture transport in the air. The complete form of this parametric function is discussed in the next section.

3. Parametric function and effective wetting coefficients

The parametric correction function and the effective wetting area coefficient are two new coefficients introduced to make the convective drying calculation practical. As given in

Eq. (24), the parametric function depends on chamber geometry, airflow rate, and the thermo-physical properties of air. Based on the solution of the model described by Eqs. (14)–(17), the complete form of this function is defined as:

$$\Phi(H,\delta,x,A,\dot{m}_{\mathrm{AIR}},\mu)=\frac{2}{\delta}\sum_{n=0}^{\infty}\frac{e^{-\frac{\lambda_n^2\mu p_{\mathrm{atm}}A}{0.622\dot{m}_{\mathrm{AIR}}}H}}{\lambda_n^2}\frac{\sin(\lambda_n x)}{\lambda_n} \quad (26)$$

By integrating Eq. (26) along the x axis, the averaged value of the parameter Φ across the wall cavity depth (δ) and for particular height (H) is obtained as:

$$\overline{\Phi}(H,\delta,A,\dot{m}_{\mathrm{AIR}},\mu)=\frac{2}{\delta^2}\sum_{n=0}^{\infty}\frac{e^{-\frac{\lambda_n^2\mu p_{\mathrm{atm}}A}{0.622\dot{m}_{\mathrm{AIR}}}H}}{\lambda_n^2} \quad (27)$$

Even when the simplest possible assumptions are made for the boundary conditions, the parametric correction function has a complex form. Nevertheless, this function opens a new field of study that could result in a simple table being produced for engineering practice (which is beyond the scope of the present study).

The coefficient K is introduced to take into account the effective wetting area of the wet face wall of the model. In real wall systems, only a portion of the wet wall surface is completely wetted, and Eq. (25) needs a coefficient that takes into account the non-uniformity of moisture distribution on the wall surface. The physical meaning of this coefficient may be explained in two ways. First, the coefficient K may represent the area of the wall that is fully wetted and normalized by the total wall surface area. Another physical interpretation is that it denotes an average wetness of the total wall surface. It may also represent averaged relative humidity of the air layers adjacent to the wet wall surface. This parameter is called *effective wetting surface area coefficient* (K), and is implemented in Eq. (25) in the following manner:

$$\Delta\dot{m}_{\mathrm{DRY}}=\dot{m}_{\mathrm{AIR}}\left[0.622\frac{Kp_{v,S}(T_{\mathrm{wall}})+\overline{\Phi}\Delta p}{p_{\mathrm{atm}}-Kp_{v,S}(T_{\mathrm{wall}})-\overline{\Phi}\Delta p}-W_{\mathrm{IN}}\right] \quad (28)$$

where $\Delta p=p_{v,\mathrm{IN}}-Kp_{v,S}(T_{\mathrm{wall}})$ denotes the driving water vapor pressure differential also modified with the *effective wetting surface area coefficient* (K).

Finally, the simple model for practical estimation of the convective drying rate on a wet wall surface within a ventilated chamber given by Eq. (28) is ready for validation with experimental data.

4. Experimental settings

A series of experimental tests have been conducted in the Building Enclosure Test Laboratory (BeTL) at the Pennsylvania State University. The main objective of the tests was to quantify the convective drying rate for a representative one-story high ventilated wall system with slot openings at the top and bottom. For that reason, a panel wall assembly 1.2 m wide and 2.4 m high was built and mounted on the counterweight balance system.

The ventilated wall cavity depth δ was fixed (50 mm). The inner wall was made of Homasote sheathing and covered with Tyvek house wrap type sheathing membrane. Two slot vent openings were located 25 mm from the top and bottom of the panel as shown in Fig. 1. The wetting system consisted of 15 sheets of moisture distribution paper, each fed by a small, separate PVC injection tube. However, the wetting system covered only 78% of the overall sheathing wall surface. The test panel was loaded with water in 3 doses, each 450 grams, at 4-hour intervals. The weight changes not associated with the Homasote sheathing layer are minimized by providing vapor tight barriers and seals at the back side of the wall assembly. The vapor barriers and seals also prevented the penetration of the moisture from the indoor air into the system. Since the wall drying is a slow dynamic process, an accurate measurement of the panel weight with respect to time was the key issue in experiment. Therefore, a counterbalance weighing system was developed with measurement accuracy of 5 grams as shown in Fig. 4. The counterbalance weight system consisted of a load cell, counterbalance weights, and a stiff balance arm. To eliminate any lateral force on the load cell, a spherical bearing roller was placed between the bottom of the test panel and the load cell. Before each test, the counterbalance system was calibrated to account for any system variation between the tests. The calibration equation was then used to recalculate the actual weight change of the panel based on the measured weight

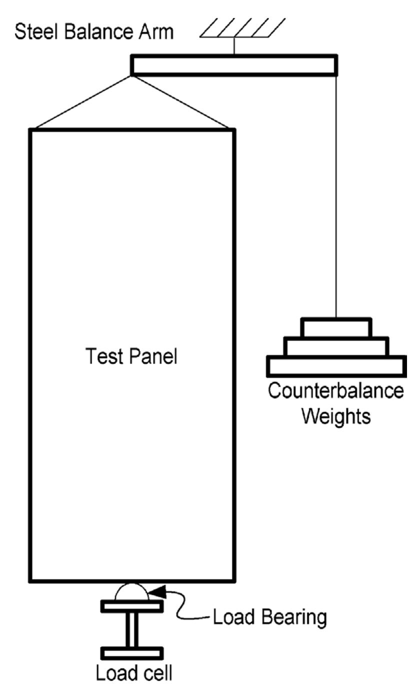

Fig. 4. The counterbalance weighing system.

change of the wall assembly. Additional details about the experimental setup are available in Ref. [17].

The objective of the experiments was to demonstrate the relationship between the drying rate and the ventilation flow rate. The drying rates were measured for four different flow rates: 1.6, 0.8, 0.4 and 0.2 $L \cdot s^{-1}$ with the reliable data currently available for 1.6 $L \cdot s^{-1}$. Field measurements identified average velocities in the ventilated wall cavity from 0.05 to 0.15 $m \cdot s^{-1}$, when the speed of approaching wind was between 1 and 3 $m \cdot s^{-1}$ [1]. For the selected range of flow rates in experiments, the averaged velocity of air in the ventilated chamber was at the lower end of the range measured in the previous field tests. A consistent airflow rate through the ventilated wall cavity represents another important aspect of the experiment. For that reason, the air was introduced into the wall assembly through the inlet manifold with flow straighteners attached with a flexible connector to the bottom vent opening. A variable speed fan with motor controller was used to provide the required flow rate of the air at the inlet vent opening. An orifice plate calibrated by laminar flow element (LFE) was used to measure the volumetric airflow rate through the system. The air was rejected into the laboratory space through the outlet pressure manifold. The outlet manifold was also connected with a flexible connector to the outlet vent opening with a zero shear resistance to avoid the influence on the panel weight measurements. The wall assembly was sealed properly to eliminate the occurrence of air leakage. The measured data were used not only to validate the proposed simple equation but also to perform analysis for both of the key model coefficients: the parametric correction function (Φ) and the effective wetting area coefficient (K).

5. Analysis of the parametric correction function Φ

The correction parametric function Φ, defined by Eq. (26), is an important coefficient in the calculation of convective drying rates. In order to keep the solution procedure simple, it is recommended that the value of the correction parametric function Φ across the cavity be averaged. An averaged value of the parametric correction function for described experimental setting was found to be $\overline{\Phi} = 0.086$. This calculation used the following parameters:

- $\dot{Q} = 1.6\ l \cdot s^{-1}$—volumetric airflow rate of air through the chamber;
- $\mu = 1.74 \times 10^{-10}$ s—water vapor permeability in the air;
- $\rho = 1.151\ kg \cdot m^{-3}$—density of the humid air (measured inlet $T = 31\,^{\circ}C$, $RH = 50\%$);
- $W = 1.2$ m—wall cavity width;
- $H = 2.4$ m—wall cavity height;
- $\delta = 0.050$ m—wall cavity depth;
- $A = W\delta$—wall cavity cross sectional area;
- $\dot{m}_{AIR} = \rho \dot{Q}$—mass flow rate of air;

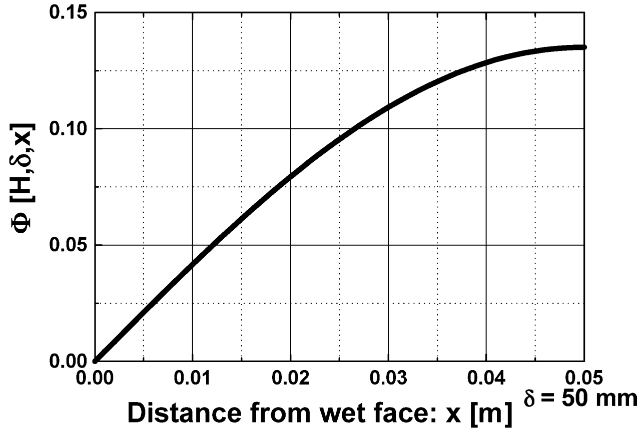

Fig. 5. The correction parametric function Φ distribution across the wall chamber at the height of outlet opening ($H = 2.4$ m) and chamber width of $\delta = 50$ mm.

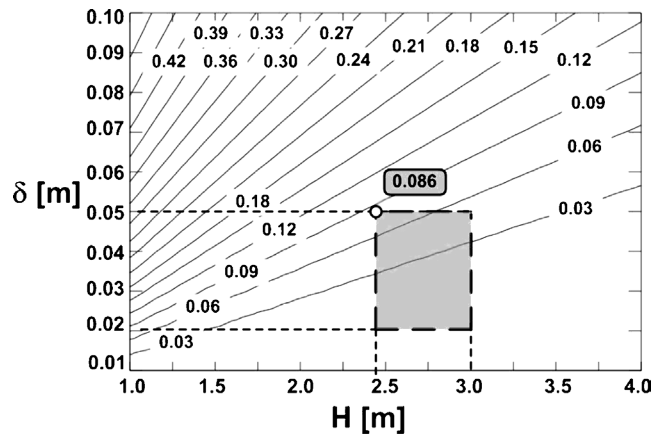

Fig. 6. The parametric correction function $\overline{\Phi}$ contour plots ($\dot{Q} = 1.6\ l \cdot s^{-1}$).

The distribution of correction function Φ across the chamber is shown in Fig. 5.

Fig. 6 shows the range of values that the parametric correction function Φ could have for different dimensions of the ventilated wall chamber and specific inlet air conditions (31 °C temperature, 50% relative humidity, and 1.6 $l \cdot s^{-1}$ airflow rate). The parametric correction function depends on the inlet air properties. The shaded area in Fig. 6 denotes the region of practical interest for design practice. The wall cavity depth (δ) for typical residential walls varies from 19 to 50 mm (3/4″ to 2 inches), and the minimum range of values for the wall height was chosen to be from $H = 2.5$ m to $H = 3.0$ m. It is evident that this area covers a range of very small values of parametric correction function Φ. Therefore, the influence of the wall cavity size is not significant for practical purposes.

The convective drying process is driven by the difference in the partial water vapor pressure across the ventilated wall chamber. The difference between the water vapor pressure in the air at the wet wall surface and the water vapor pressure of the incoming air represents the driving force for convective drying. The proposed model, Eq. (27), could also be used to

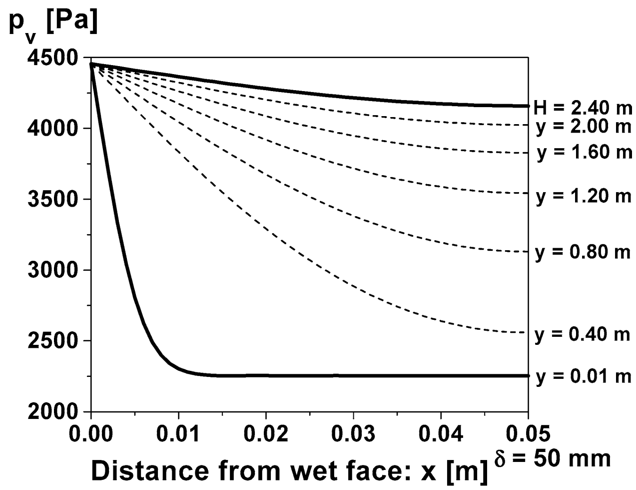

Fig. 7. Partial water vapor distribution in air across the wall cavity for different wall heights ($\dot{Q} = 1.6\ \mathrm{l \cdot s^{-1}}$; $\delta = 50$ mm; $H = 2.4$ m, $t_{\mathrm{wall}} = 31\,^{\circ}\mathrm{C}$, $t_{\mathrm{IN}} = 31.2\,^{\circ}\mathrm{C}$, $\varphi_{\mathrm{IN}} = 50\%$).

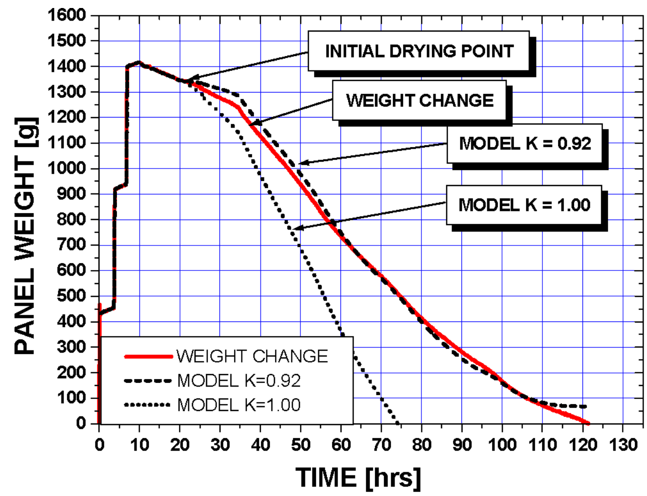

Fig. 8. Modeled and measured experimental drying curves ($\dot{Q} = 1.6\ \mathrm{l \cdot s^{-1}}$; $\delta = 50$ mm; $H = 2.4$ m; $\Phi = 0.086$).

calculate the profiles of the partial water vapor pressure for the measured airflow rate and the drying rate, as shown in Fig. 7. Different profiles are calculated for different heights in the wall cavity, namely, 0.01 m (inlet region), 0.4, 0.8, 1.2, 1.6, 2.0, and 2.4 m (outlet region). As expected, the model gives the highest water vapor pressure gradient at the inlet region and the lowest value at the outlet region. In other words, the largest potential for convective drying occurs at the inlet region of the wall system. As the air stream approaches the outlet, its water vapor content increases, resulting in decreased convective drying potential and smaller gradients of water vapor pressure profiles respectively.

6. Analysis of the effective wetting coefficient K

In order to validate the theoretical model, it was necessary to compare the calculated results with measured data. Fig. 8 shows a comparison between the drying curves plotted using the proposed model equation and the curve obtained in the experimental measurements of the wall assembly expressed as the change in weight of the wall panel. The proposed steady-state, two-dimensional, model equation is applied to the time-dependent drying process in the following way. The equation was used at five-minute intervals to calculate the convective drying rate and the amount of moisture removed from the panel wall assembly. This value was subtracted from the amount of moisture stored in the wall system during the previous time step. The same sampling rate was used to measure the weight change of the wall panel assembly during the experiments. The measured inlet air conditions and the conditions at the wet wall surface were used as input values for each time step in the model equation.

The model equation also uses the two coefficients, the parametric correction function and the effective wetting surface area coefficient, which are not time dependent. As previously stated, the calculated average value of the parametric correction function Φ is 0.086. The effective wetting surface area coefficient K was originally assumed to be 0.78 to match the ratio of the wetting system surface to the sheathing wall surface ratio in experiments. However, the adopted K value resulted in a significantly different drying rate when compared to the actual measured panel weight. The refinement process of the effective wetting surface area coefficient resulted in the value $K = 0.92$, which agrees very well with the experimental curve. Overall, the model shows high sensitivity to the coefficient K, which is quite different behavior from the parametric correction function Φ.

The analysis conducted for the proposed simple analytical model for the convective drying rate within a ventilated wall chamber revealed several very important issues. Fig. 6 shows the range of possible values for the correction parametric function Φ to be between 0.007 and 0.09 approximately. The values lower then 0.03 are omitted from Fig. 6 due to dense distribution of contour lines for the small Φ values. The significantly higher values of this coefficient exist only for very large values of ventilated wall cavity depths (δ), and relatively small heights (H). In real wall systems, the averaged value of this correction parametric function is rarely larger than 0.2 assuming that wall cavity depth may take the values up to 75 mm (2 inches). For practical applications, it is justifiable to use a single constant value of the correction parametric function. The simplest approach would be to adopt a single value for Φ in the proposed range. On the other hand, if an accurate calculation is required, the parametric function distribution should be integrated across the chamber depth. Finally, the average value along the chamber height should be calculated based on the integral values.

The chamber height is an important parameter for the convective drying process performance. In general, larger wall chamber heights are recommended to increase the driving pressure differential for ventilation due to the thermal stack effect. In this study, the partial water vapor pressure profiles close to the outlet opening are almost flat, as shown in Fig. 7. The flat water vapor profile indicates that the drying rates, both by water vapor diffusion and convection, in the upper parts of the ventilated wall chamber are negligible. There is even a possibility for rewetting to occur in the outlet region, caused by the redistribution of moisture from the lower to the upper parts of the ventilated wall chamber. The moisture is likely to be located mainly in the lower regions of the chamber due to gravity effects. Therefore, assuming the upward airflow direction, the transport of moisture may occur from the lower to the upper wall surface due to convective moisture transport by the air flowing through the ventilated chamber. It is also possible to have the air flow through the system directed downwards, and in that case the moisture redistribution would not occur.

In the experiments performed by Schumacher et al. [17], the airflow direction was oriented upwards; therefore, the wetting process of the upper part of the wall surface could occur. In fact, the determined value for K ($K = 0.92$), shows that the redistribution of the moisture probably occurred during the process of the moisture transport from the wetting system to the rest of the Homasote sheathing. Therefore, the effective wetting surface area coefficient has value of 0.92, although the wetting system covered only 78% of the sheathing wall surface. Another reason for the increase of K may be the fact that the effective wetting surface area coefficient K takes into account only the uniformly distributed moisture on the wall surface, neglecting the non-uniformity of the airflow. This issue may be of great importance, especially in the corner zones, inlet and outlet regions of vent openings. Further improvement of the proposed model may take these factors into account.

The modeled and experimental curves show discrepancy at the very end of the drying process ($K = 0.92$). According to the proposed model equation, the drying process asymptotically goes to zero, while the experimental results show an asymptotic behavior different from the zero value for moisture content. This behavior could be explained either by approximations in the model introduced with assumption for constant K value, or due to experimental instrumentation inaccuracy. At the end of the drying process the difference between inlet and outlet water vapor pressures becomes negligible causing the measurement readings for temperature and relative humidity to become more unreliable. The sensitivity and the accuracy of measuring sensors, especially for relative humidity, may play a significant role in the accurate evaluation of the convective drying rates in conditions of extremely low airflow rates. The sensitivity analysis revealed that the measurements of the humidity ratio cause the largest uncertainty for the experimental results. The accuracy of relative-humidity ratio measurements is $\pm 2\%$, creating enormous variations in the drying curve at the end of the drying process. Nevertheless, the main drying process predicted by the model equation and the measurements agree very well.

7. Conclusions

An analytical equation was derived for practical estimation of convective drying in ventilated wall chambers, commonly installed in North America for prevention of mold problems in residential housing. The model derivation included several practical assumptions based on experience with outdoor conditions in real wall chambers. The proposed simple model equation was applied to the experimental conditions and compared to the experimentally obtained drying curve. The calculation results and experimental data exhibit very good agreement after the adjustment of the effective wetting surface area coefficient K. The ventilated wall chamber geometry (aspect ratios and heights) has little influence on the drying process for typical dimensions of the ventilated chambers based on the model parametric study. Introduced model coefficients, the parametric correction function Φ, and the effective wetting surface area coefficient K need further parametric studies to establish a coefficient database for engineering practice. A data library should be developed by experimental measurements and numerical simulations.

The model equation can be applied to dynamic drying process with changing outdoor boundary conditions, although it was derived for the steady-state drying process. In fact, the equation performed well for the transient drying processes when applied in small time increments such as five minutes. It is also possible to use the equation for different scenarios of moisture transport, either through the cladding wall or through the inner portion of the wall system, resulting in a universal model. The practical importance of this equation lays in its easy implementation and applicability to engineering design calculations of drying performance for the ventilated wall systems. Future validation with on-site experiments is necessary.

Acknowledgement

The project was sponsored by the National Science Foundation (NSF), Grant award #0122062.

References

[1] J. Straube, E.F.P. Burnett, Vents, Ventilation Drying and Pressure Moderation, Building Engineering Group, University of Waterloo, Canada, 1995.
[2] A.V. Luikov, Heat and Mass Transfer in Capillary-Porous Bodies, Pergamon, New York, 1966.
[3] C.E. Hagentoft, Introduction to Building Physics, Studentlitteratur, Lund, 2001.
[4] H.R. Trechsel, Moisture Analysis and Condensation Control in Building Envelopes, ASTM Manual Series, ASTM, Philadelphia, PA, 2001.
[5] I. Turner, A.S. Mujumdar, Mathematical Modeling and Numerical Techniques in Drying Technology, Marcel Dekker, New York, 1997.
[6] D. Davidovic, Convective drying potential of ventilated wall cavity systems in building enclosures, MSc thesis, Department of Architectural Engineering, The Pennsylvania State University, 2004, 255 p.

[7] A.V. Luikov, Heat and Mass Transfer, Mir, Moscow, 1980.
[8] D. Saelens, H. Hens, Experimental evaluation of airflow in naturally ventilated active envelopes, J. Thermal Env. Bldg. Sci. 25 (2001) 101–127.
[9] V.S. Arpaci, P.S. Larsen, Convection Heat Transfer, Prentice-Hall, Englewood Cliffs, NJ, 1984.
[10] A. TenWolde, Steady-state one-dimensional water vapor movement by diffusion and convection in a multilayered wall, ASHRAE Trans. 91 (1985) 332–341.
[11] ASHRAE, ASHRAE Handbook: Fundamentals 2001, American Society of Heating, Refrigerating, and Air-Conditioning Engineers, Atlanta, GA, 2001.
[12] J.S. Farlow, Partial Differential Equations for Scientist and Engineers, Wiley, New York, 1982.
[13] H.S. Carslaw, J.C. Jaeger, Conduction of Heat in Solids, Clarendon Press, Oxford, 1959.
[14] A.G. Hansen, Similarity Analyses of Boundary Value Problems in Engineering, Prentice-Hall, Englewood Cliffs, NJ, 1964.
[15] M.N. Öziik, Heat Conduction, second ed., Wiley, New York, 1993.
[16] V.S. Arpaci, Conduction Heat Transfer, Addison-Wesley Series, Addison-Wesley, Reading, MA, 1966.
[17] C. Schumacher, X. Shi, D. Davidovic, E. Burnett, J. Straube, Ventilation drying in wall systems in: Second International Building Physics Conference, Leuven, Belgium, September 14–18, 2003.